1. Michał GOŁĄBEK[1], 2. Bartłomiej BARAN[1], 3. Piotr BOŻEK[1],
4. Daria STEFAŃCZAK[1], 5. Dariusz WÓJCIK[1,2]

Research and Development Center, Netrix S.A. (1), University of Economics and Innovation (2)
ORCID: 1. 0000-0002-2696-505X; 2. 0000-0001-9544-3696; 3. 0000-0003-4929-1251; 4. 0009-0003-6297-3473; 5. 0000-0002-4200-3432;

doi:10.15199/48.2024.04.48

Design features of a portable ultrasonic-impedance tomograph for bladder monitoring

***Abstract**. This paper describes the construction of an ultrasonic tomograph combined with an impedance tomograph for bladder monitoring. The combination of both tomography techniques allows for an increase in the accuracy of urinary tract imaging. The main advantages of a dual tomographic system are the non-invasiveness, low cost of production and small size. The device supports the ultrasound beamforming technology and makes measurements using a phased array ultrasonic transducer. The impedance measurement device uses electrodes made of conductive material placed directly on the body.*

***Streszczenie.** W artykule opisano budowę tomografu ultradźwiękowego połączonego z tomografem impedancyjnym do monitorowania pęcherza moczowego. Połączenie obu technik tomografii pozwala zwiększyć dokładność obrazowania dróg moczowych. Głównymi zaletami podwójnego systemu tomograficznego jest bezinwazyjność, niski koszt produkcji i niewielkie rozmiary. Urządzenie obsługuje technologię ultradźwiękowego kształtowania wiązki i wykonuje pomiary za pomocą głowicy ultradźwiękowej typu phased array. Do pomiaru impedancji urządzenie wykorzystuje elektrody wykonane z materiału przewodzącego, umieszczane bezpośrednio na ciele (**Cechy konstrukcyjne przenośnego tomografu impedancji ultradźwiękowej do monitorowania pęcherza moczowego**).*

Keywords: ultrasound tomography, electrical impedance tomography, beamforming, bladder monitoring
Słowa kluczowe: tomografia ultradźwiękowa, tomografia impedancyjna, formowanie wiązki, monitorowanie pęcherza

Introduction

Urinary system abnormalities are a notable concern among children, with estimates indicating their impact on over 20% of children and 2-4% of adolescents below five [1-2]. These anomalies can be linked to diverse urinary tract irregularities, bowel movement difficulties, and central nervous system disorders like spina bifida and cerebral palsy [3]. Nevertheless, many children may solely experience functional issues, which pose challenges in accurate diagnosis and effective management due to the absence of affordable, non-intrusive diagnostic techniques that offer a comprehensive functional assessment of the urinary system [2].

The purpose and motivation of the conducted research was to create a low-cost and convenient device for effective diagnosis and treatment of urinary system abnormalities in children and adults. The prepared article discusses the technical issues of the designed device.

Tomograph construction

The design of the measuring device for dual diagnosis of the urinary tract is divided into several PCB boards. It consists of the mainboard, four ultrasounds measurement cards (UST), one impedance measurement card (EIT) and LED board for operation status indication.

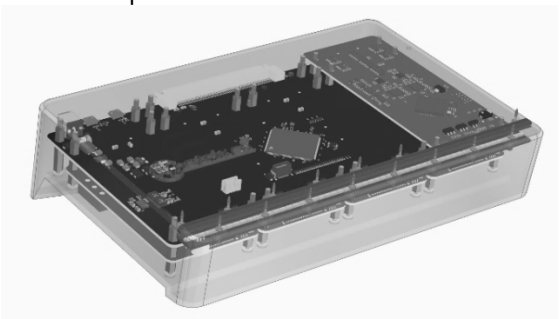

Fig.1. 3D model of UST & EIT tomograph construction

The mainboard was based on the STM32H7 microcontroller. It supports parallel FMC data transmission operating at 100MHz clock from ultrasonic measurement cards and provides communication with the impedance measurement card using UART and QUAD SPI. In addition, the motherboard has USB 1.0 and USB 2.0 communication ports for connection to the image reconstruction system. The motherboard also provides the appropriate supply voltage levels to the individual modules.

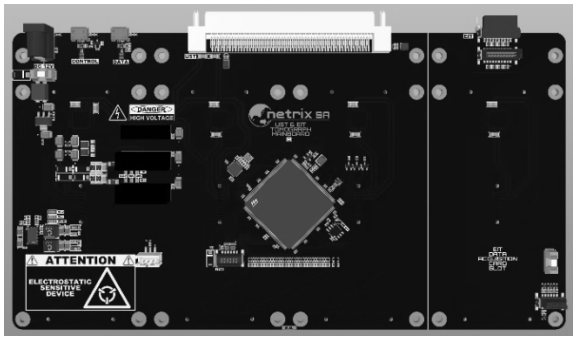

Fig.2. Mainboard of a portable ultrasonic-impedance tomograph for bladder monitoring

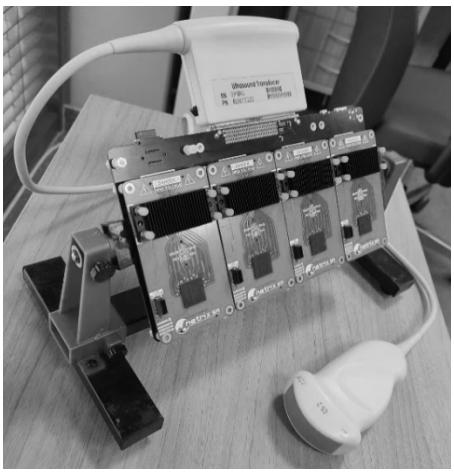

Fig.3. Assembled tomograph mainboard

The board was made in six-layer copper and was manufactured on 2mm thickness PCB to ensure the best separation of high-voltage signals from connected ultrasound measurement cards.

Each UST measurement card has eight measurement channels, which gives 32 measurement channels. The motherboard also has built-in 2:1 multiplexers, allowing UST channels to multiply up to 64. The UST cards are synchronized with each other by a common clock, which allows control of the excitation on each channel with an accuracy of up to 1ns. This feature is required for ultrasound beamforming measurements.

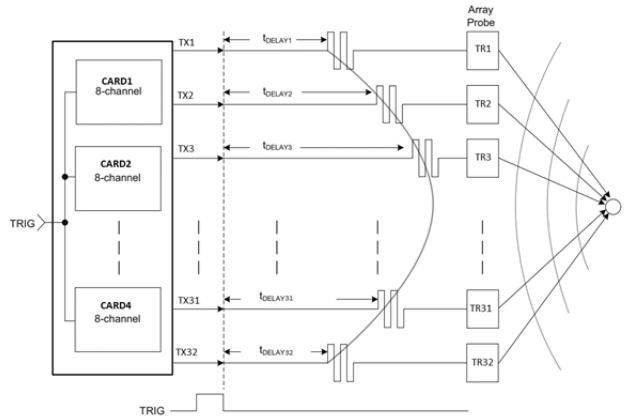

Fig.4. Ultrasonic beamforming implementation.

Beamforming technology gives the ability to perform a large number of reflection measurements using a small number of channels/transducers (and their number is mainly due to the step with which the phase of the transmitting signal will be shifted). The phase shift on each of the transmitting transducers allows the direction of the wave beam at a specific angle, thanks to which, using static transducers, it is possible to image similarly as using one transducer with a mechanically controlled angle/direction. Beamforming also allows the focus of the ultrasonic wave at a point, making it possible to inspect the object sector by sector [4].

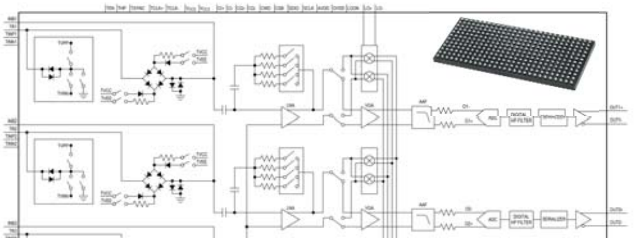

Fig.5. Part of internal schematic of MAX2082 from Analog Devices[16]

The UST measurement card includes an octal-channel measurement integrated circuit MAX2082 from Analog Devices [Fig. 5] and FPGA Altera Cyclone IV from Intel. The MAX2082 contains 8x High Voltage 3-Level 2A Pulsers, 8x T/R switchers, 8x Low Noise Amplifiers (LNA), 8x Variable Gain Amplifiers (VGA), 8x anti-aliasing filters (AAF), 8x ADC 12 bit 50 MSPS and 8x Digital High Pass Filters.

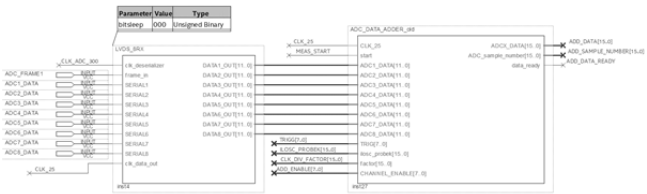

Fig.6. Implementation of measurement data deserialization alignment in phase and summation

The above figure shows the data acquisition method from a single MAX2082 chip. The phase-shifted measurement data are deserialized in the first block with the 300MHz clock from the MAX2082 chip. Using a 25MHz clock, data from 8 ADCs are fed simultaneously to the summation block. Based on the table of delays for eight channels, this block receives eight trigger signals (TRIG[7..]), which sums up data from all channels with a given delay. The summed output data (ADCX_DATA[15..0]) are transferred to the FPGA's internal RAM, from where, using the FMC bus, they are loaded to the STM32H7 microcontroller along with data from other measurement cards, where the already completed data are added up, as a result of which the result of a single sample measurement is 17 bits. The number of measurements per one measurement matrix is set with the parameter ILOSC_PROBEK[15..0], this number is 16-bit, but due to the limited amount of RAM available in the FPGA and the STM32H7 microcontroller, this number is limited to 16000 measurements.

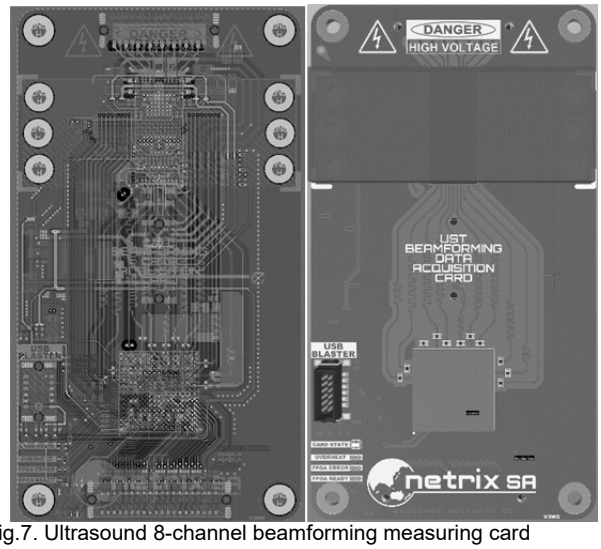

Fig.7. Ultrasound 8-channel beamforming measuring card

Before the measurements, the UST cards are parameterized by the main board. They send data about delays on each channel, the number of measurement samples, excitation frequency, pulses, filtering and active channels. The common clock and the low state on GPIO trigger line are responsible for the accurate synchronization of the start of measurements. The collected data are summed up based on the delay data to one common 16-bit measurement vector and sent via FMC and USB to the reconstruction image system.

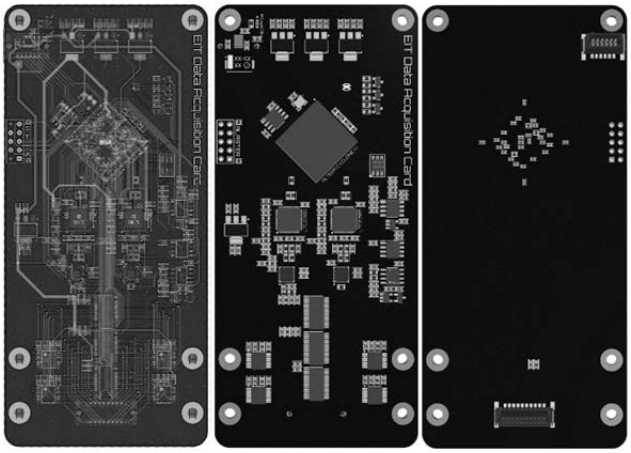

Fig.8. Electrical impedance 16-channel measuring card

The EIT measurement card provides impedance measurements using 16 wearable textile electrodes made of conductive material. The voltage and current values are measured using the ADC converter system from Linear Technology LTC2203, which has a sampling rate of up to 25Msps and uses a pipelined architecture with a built-in PGA. Data transmission to the FPGA is done using a parallel bus. Current excitation is achieved using digital-to-analog converters. The FPGA system controls two DAC8830 converters using a serial bus. The converters work concurrently, with one converter's output being used as a reference signal for the other. This enables the system to generate any waveform shape while maintaining the necessary resolution for digital amplitude control.

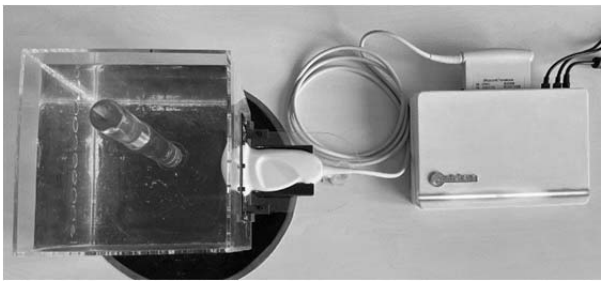

Fig.9. Assembled portable ultrasonic-impedance tomograph for bladder monitoring with Philips Convex ultrasound phased array 128 channel transducer C5-2

Measurement sensors

The task aimed to develop measuring sensors for ultrasonic and impedance tomography and the method of their assembly on the patient's body. Both of these goals have been achieved. The developed solution is based on a measuring insert mounted in textile underwear.

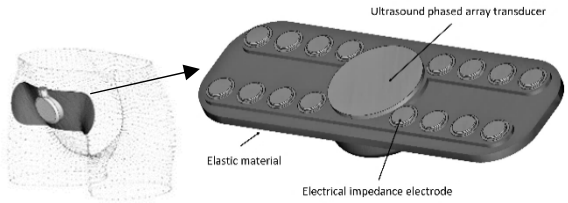

Fig.10. Elastic insole with UST small phased array transducer and EIT measuring sensors

This solution allows using the measuring sensor with underwear in different sizes. The pocket on the underwear fixes the measuring sensor at the level of the bladder. The pressure of the sensor on the patient's body is carried out using Velcro tapes, which also allows for a better fit of the underwear to a wide range of patients with different anatomy.

Fig.11. Textile underwear with Velcro fasteners for attaching the measuring insert to the patient's body

For the measuring insert presented above was made a dedicated ultrasonic transducer. The transducer has been adapted to the hole inside the measuring insert and made with attention to the smallest possible size. Parameters were matched to bladder imaging. The head used has a linear 32-channel array of transducers made with a 500um pitch, with a max focusing depth of 13 cm, approx. and steering angle +/-30°.

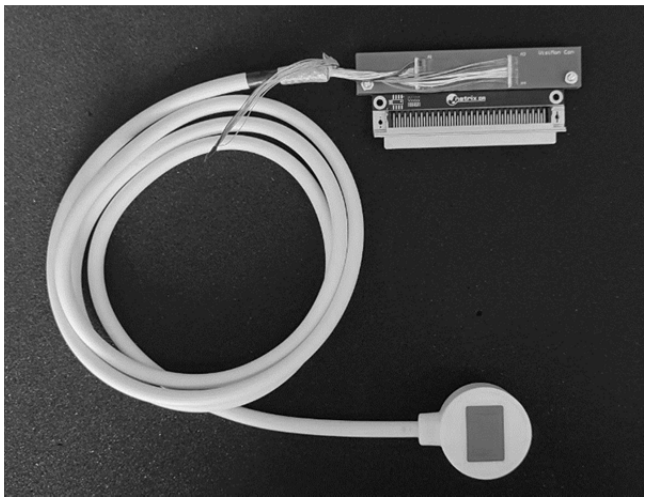

Fig.12. Dedicated 32-channel linear measuring ultrasound phased array transducer with a center frequency of 3MHz

Measurements

The device's measurement sequence strictly depends on the tested object and the connected UST measuring probe. Based on the geometry of the probe and the examined area, it should be assumed how many measurements will be sufficient to perform image reconstruction. The simplest and fastest measurement sequence consists of as many vectors as the ultrasonic head of piezoelectric elements. In the case of a 128-channel head, the device can perform 128 measurements from each piezoelectric element separately without beamforming technology, allowing for image reconstruction in the shortest time and in the poorest quality. Image quality can be significantly improved by compacting the measurement vectors by changing the direction of ultrasonic wave propagation.

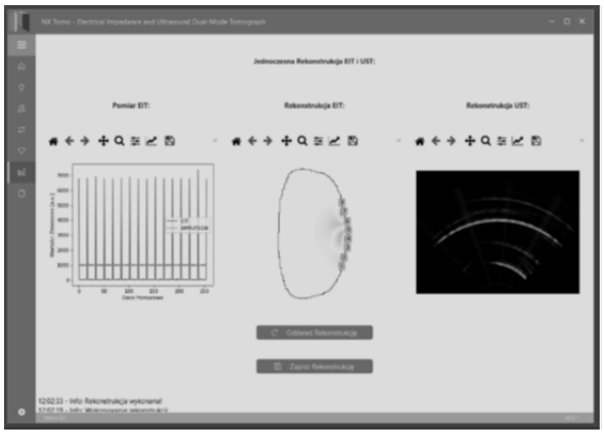

Fig.13. Image reconstruction system with EIT measurements results on left side and UST measurements results on right side

Many different methods are used to analyze data [5-17]. Figure 14 illustrates the results of different imaging techniques applied to a medical phantom visible on the left top panel display. The right top panel shows the reconstructed bladder using the B-mode algorithm in ultrasound tomography (UST), while the right bottom panel shows the reconstruction obtained using the Philips Lumify

system for comparison. The left bottom panel presents the differential reconstruction of electrical impedance tomography (EIT), specifically the measurement difference between a filled and empty bladder. The reconstruction was obtained using the Damped Gauss-Newton method with a regularization constant (λ) set to 1e-9.

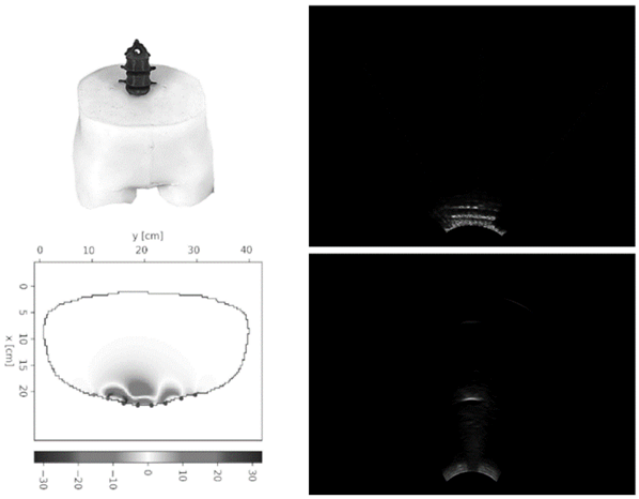

Fig.14. Reconstructions results

Metrics such as Peak Signal-to-Noise Ratio (PSNR) and Structural Similarity Index (SSIM) coefficients were calculated to evaluate the quality of the results obtained with the original device. Based on the average values of these coefficients from 24 measurements, the PSNR was determined to be 29.45 (with a standard deviation of 0.27), and the SSIM was found to be 0.65 (with a standard deviation of 0.01).

Discussion and summary

In conclusion, the paper presents the design features of a bimodal tomograph for examining the lower urinary tract, enabling simultaneous ultrasound and impedance imaging. The combination of both measurement techniques allowed to increase the accuracy of imaging. Both tomographs are non-invasive for patients. The collected test results show that the designed system will provide the necessary information to diagnose lower urinary tract diseases. The presented design solutions will be constantly improved and will ensure much better mobility, low cost, and better access to urological examinations. We anticipate that our device will streamline the treatment of urological diseases and facilitate the planning individualized therapies for patients.

***Authors**: Michał Gołąbek, Research & Development Centre Netrix S.A. Związkowa 26, Lublin, Email: michal.golabek@netrix.com.pl; Bartłomiej Baran, Research & Development Centre Netrix S.A. Związkowa 26, Lublin, Email: bartlomiej.baran@netrix.com.pl; Piotr Bożek, Research & Development Centre Netrix S.A. Związkowa 26, Lublin, Email: piotr.bożek@netrix.com.pl; Daria Stefańczak, Research & Development Centre Netrix S.A. Związkowa 26, Lublin, Email: daria.stefanczak@netrix.com.pl; Dariusz Wójcik, University of Economics and Innovation, Projektowa 4, Lublin, Poland/ Research & Development Centre Netrix S.A. E-mail: dariusz.wojcik@netrix.com.pl;*

REFERENCES

[1] Kathrin Heilenkütter, Christian Bachmann, Ellen Janhsen, Tatiana Stauber, Hildegard Lax, Franz Petermann, and Hannsjörg Bachmann. *Prospective evaluation of inpatient and outpatient bladder training in children with functional urinary incontinence*. Urology, 67(2006), No. 1, 176–180.

[2] Daniela Schultz-Lampel, Christian Steuber, Peter F. Hoyer, Christian J. Bachmann, Daniela Marschall-Kehrel, and Hannsjörg Bachmann. *Urinary incontinence in children*. Deutsches Ärzteblatt international, September 2011.

[3] Wang, J.Y.; Liao, L.; Liu, M.; Sumarsono, B.; Cong, M. *Epidemiology of lower urinary tract symptoms in a cross-sectional,population-based study*. Medicine, (2018), 97, e11554.

[4] Giulia Matrone, Alessandro Stuart Savoia, Giosue Caliano, and Giovanni Magenes. *The delay multiply and sum beamforming algorithm in ultrasound b-mode medical imaging*. IEEE Transactions on Medical Imaging, 34(2015), No. 4, 940–949.

[5] Kania, W., Wajman, R., Ckript: a new scripting language for web applications, Informatyka, Automatyka, Pomiary W Gospodarce I Ochronie Środowiska, 12(2022), No. 2, 4-9.

[6] Lebioda, M., Korzeniewska, E., The Influence of Buffer Layer Type on the Electrical Properties of Metallic Layers Deposited on Composite Textile Substrates in the PVD Process, Materials, 16 (2023), No. 13, 4856.

[7] Koulountzios P., Rymarczyk T., Soleimani M., A triple-modality ultrasound computed tomography based on full-waveform data for industrial processes, IEEE Sensors Journal, 21 (2021), No. 18, 20896-20909.

[8] Koulountzios P., Aghajanian S., Rymarczyk T., Koiranen T., Soleimani M., An Ultrasound Tomography Method for Monitoring CO2 Capture Process Involving Stirring and CaCO3 Precipitation, Sensors, 21 (2021), No. 21, 6995.

[9] Styła, M., Adamkiewicz, P., Hybrid navigation system for indoor use. Informatyka, Automatyka, Pomiary W Gospodarce I Ochronie Środowiska, 12 (2022), No. 1, 10-14.

[10] Sikora R., Markiewicz P., Korzeniewska E., Using identification method to modelling short term luminous flux depreciation of LED luminaire to reducing electricity consumption, Scientific Reportst, 13 (2023), No. 1, 673.

[11] Rymarczyk T., Kozłowski E., Kłosowski G., Electrical impedance tomography in 3D flood embankments testing – elastic net approach, Transactions of the Institute of Measurement and Control, 42 (2020), No. 4, 680-690.

[12] Kłosowski G., Rymarczyk T., Niderla K., Rzemieniak M., Dmowski A., Maj M., Comparison of Machine Learning Methods for Image Reconstruction Using the LSTM Classifier in Industrial Electrical Tomography, Energies 2021, 14 (2021), No. 21, 7269.

[13] Rymarczyk T., Kłosowski G., Hoła A., Sikora J., Tchórzewski P., Skowron Ł., Optimising the Use of Machine Learning Algorithms in Electrical Tomography of Building Walls: Pixel Oriented Ensemble Approach, Measurement, 188 (2022), 110581.

[14] Kłosowski G, Rymarczyk T, Niderla K, Kulisz M, Skowron Ł, Soleimani M., Using an LSTM network to monitor industrial reactors using electrical capacitance and impedance tomography – a hybrid approach. Eksploatacja i Niezawodnosc – Maintenance and Reliability, 25 (2023), No. 1, 11.

[15] Kłosowski G., Rymarczyk T., Kania K., Świć A., Cieplak T., Maintenance of industrial reactors supported by deep learning driven ultrasound tomography, Eksploatacja i Niezawodnosc – Maintenance and Reliability; 22 (2020), No 1, 138–147.

[16] Leonhäuser, D.; Castelar, C.; Schlebusch, T.; Rohm, M.; Rupp, R.; Leonhardt, S.; Walter, M.; Grosse, J.O. *Evaluation of electrical impedance tomography for determination of urinary bladder volume: Comparison with standard ultrasound methods in healthy volunteers*. Biomed. Eng. Online, 17 (2018), 95.

[17] Maserejian, N.N.; Chen, S.; Chiu, G.R.; Wager, C.G.; Kupelian, V.; Araujo, A.B.; McKinlay, J.B. Incidence of lower urinary tract symptoms in a population-based study of men and women, Urology. 2013 Sep; 82 (2013), No.3, 560–564.